DESIGN OF A BEAMFORMING NETWORK USING BUTLER MATRIX

MOHAMAD ZOINOL ABIDIN BIN ABD AZIZ

RESEARCH VOTE NO:
PJP/2006/FKEKK (4) – S192

FACULTY OF ELECTRONIC ENGINEERING AND COMPUTER ENGINEERING
UNIVERSITI TEKNIKAL MALAYSIA MELAKA

2007

Design of a Beamforming Network Using Butler Matrix

(Keyword: smart antenna, beamforming network, Butler Matrix, MIMO)

Nowadays, communication systems are moving towards higher data rate transmission. MIMO is one of the techniques which is new and widely explore by the researchers. MIMO concept can achieve by implement Beamforming Network into the system. This paper describes the design, simulation and fabrication of a 4 x 4 Butler Matrix for the 2.4 GHz (WLAN). A Butler Matrix is a multiport component which when loaded with radiating elements enables production of a beam of microwave energy in a specified direction in transmission line, dependent upon which input port is activated. The circular and mitered bends was applied in designing the beamforming network based on Butler Matrix technique. Results from simulation and fabrication is then being compared in term of return loss (S_{ii}), transmission coefficient (S_{ji}), isolation (S_{ij}) and the phase difference (β) between each port (4x4). The measurement patterns result achieved by this project is then compared with the simulation result. The design has been measured by using Advantest R3767 Network Analyzer.

Key Researchers:
Mohamad Zoinol Abidin B. Abd Aziz

Email : mohamadzoinol@utem.com.my
Tel. No. : 06-5552130
Vote No. : PJP/2006/FKEKK(4) - S192

ACKNOWLEDGMENTS

Praise is to Allah who has give me the strength, physically and mentally in order for me to complete this project.

I would like to take this opportunity to thank University Industry Center (UNIC) of UTeM for funding and assisted me in this project. The thanks goes also to my co-researcher, Mr. Imran Bin Ibrahim and Mr. Abd. Shukur Bin Ja'afar for their support in this project. I would like also to thank my co-supervission master student, Mr. Muhammad Rafie Bin Che Rose and Microwave Lab Technician, Mr. Mohd Aeini Bin Amin for their work and help that is valuable to the project. Special thanks also go to all UTeM staff, which are direct or indirectly support this project.

Lastly, I would like to acknowledge, with many thanks, my entire friend and whoever involved that contributed to the successful of this project.

TABLE OF CONTENT

LIST OF ABREVIATION

a	-	Side length
a_{eff}	-	Efficiency Value of Side Length
AS	-	Angular Spread
BW	-	Bandwidth
BFN	-	Beamforming Network
BM	-	Butler Matrix
d	-	Substrate Thickness
dB	-	Decibel
Degs / °	-	Degree
DG	-	Diversity Gain
ESA	-	European Space Agency
Freq	-	Frequency
FR4	-	Flame Retardant 4
GHz	-	Giga Hertz
IEEE	-	Institute of electrical and Electronic Engineering
ISM	-	Industrial, Scientific and Medical
km	-	Kilometer
Log	-	Logarithm
LOS	-	Line of Sight
Mag	-	Magnitude
MEA	-	Multi Element Antenna
MHz	-	Mega Hertz
MIMO	-	Multiple Input Multiple Output
mm	-	Millimeter
MPA	-	Multiport Power Amplifier
MWO	-	Microwave Office 2004
P	-	Power
PCB	-	Printed Circuit Board
RF	-	Radio Frequency

RL	-	Return Loss
Rx	-	Receiver
SD	-	Selection Diversity
SNR	-	Signal to Noise Ratio
T	-	Conductor Thickness
Tan δ	-	Tangent Loss
Tx	-	Transmitter
V	-	Voltage
W	-	Width
WLAN	-	Wireless Local Area Network
Z	-	Impedance
Z_o	-	Characteristic Impedance
θ	-	Phase
ε_r	-	Effective Dielectric
ε_{eff}	-	Effective Permittivity
ℓ	-	Length
π	-	Phi
λ	-	Wavelength
λg	-	Waveguide
3-D	-	3 Dimension

LIST OF FIGURES AND TABLES

1.0 INTRODUCTION

In recent years wireless local area networks have experience increasing popularity. As business and home users continue to demand high data rates with continued network complexity. The Butler Matrix consists of an equal number of input and output ports connected through an array of phase shifters and couplers such that when a signal is applied to any input port it produces equal amplitude signals at all output ports. Figure 1 shows the block diagram of the 4x4 Butler Matrix.

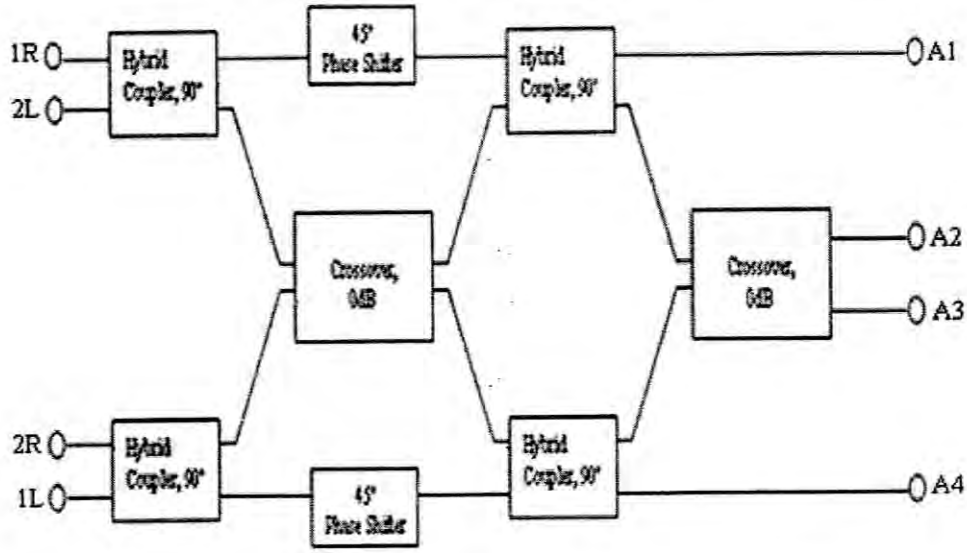

Figure 1.1: Block Structure of a 4 x 4 Butler Matrix

The beamforming network is a network that controls the phases and amplitudes of the excitation current for smart antennas. A signal processor will control which port of the beamforming network is used to feed or receive signals while the beamforming network will feed the signal to an array of antennas [2]. The advantages of Butler Matrix are their simplicity and easy fabrication characteristics. Butler matrix is used widely in antenna feed applications in beamforming networks, multiport power amplifiers, adaptive smart antenna systems for direction finding purposes and in satellite communication applications. [3]

The circular and mitered bend designs for the beamforming network are developed. The transmission lines in circular bend has been placed far from each other while for mitered bend, it is placed closely. This is to determine the coupling effect of transmission line proximity. The output ports for circular bend have been spaced in such a way that antennas can be attached directly to the network. The output ports for circular bend have been spaced in such a way that antennas can be attached directly to the network [1]. Microwave Office 2003 software will be used to simulate both designs. The prototype is fabricated on FR4 board with the effective dielectric being 4.7, substrate thickness, 1.6 mm, and the dissipation loss, 0.019.

2.0 PROBLEM STATEMENTS

In applications where size, weight, cost, performance, ease of installation, and aerodynamic profile are constrains, low profile antennas like micros trip antennas are required. Because micros trip inherently has narrow bandwidths (BW) and in general, are half-wavelength structures operating at the fundamental resonant mode researchers have made efforts to overcome the problem of narrow bandwidth. [1]

Traditionally, a wideband antenna in the low frequency wireless bands can only be achieved with heavily loaded wire antenna, which usually means different antennas are needed for different frequency bands. And this will increased the cost to developing the antenna. [2] The high expense of implementing the multiple RF chains motivates the recent popularity of antenna selection schemes. [9]

3.0 PROJECT OBJECTIVE

These project objectives are to design, simulate and fabricate a 4 x 4 Butler Matrix by using Beamforming network. The designs require transmission line such as width and length, isolation and return loss in a specified at 2.4 GHz. Finally, the design Beamforming network should work properly in the Wireless Local Area Network (WLAN) environment.

4.0 SCOPE OF PROJECTS

This project consists of an eight phases. For the first phase, study the concept of beamforming network and butler matrix technique. In order to understand all the basic theory and concept of the related topic of this project, some research were made in Beamforming network using design 4 x 4 Butler Matrix technique and exploring the function of Microwave Office 2004. All the material that related to the beamforming, MIMO, butler matrix and other related this project in books, journals and articles have been collected.

The design parameters such as transmission line such as width and length will be calculated. Then, the 4 X 4 Beamforming network circuit will be simulate by using Microwave Office 2004. The coupling coefficient, isolation and phase difference for each port have been simulated. Then, the designs have been fabricated by using an etching technique. The prototypes have been measured and the results have been compared with the simulation result.

5.0 DESIGN METHODOLOGY AND SOFTWARES

Several methodologies have been employed and need to be understood thoroughly. This chapter covers the methods that will be used and the software needed to perform simulating processed the project and preparation for fabrication processed.

5.1 Design Methodology

Figure 3.1 shows the flowchart which describes the methods that have been used in this project. The first step in designing the beam forming network using Butler Matrix requires an understanding of its design procedures. The basic layout of the BFN will be designed. Then, the focus will be on designing each component of the BFN. The detail studies on each component have been done. Then the relevant equation and specification have been determined. The design simulation process has been done by using Microwave Office software. The designs have been fabricated on a FR4 board. CorelDRAW Graphic Suite 12 has been used to transform the circuit from Microwave Office into a layout printable on a transparency.

The designed prototypes have been measured by using Network Analyzer Spectrum Analyzer at the FKEKK, UTeM. The measurement results have been compared to the simulation processed.

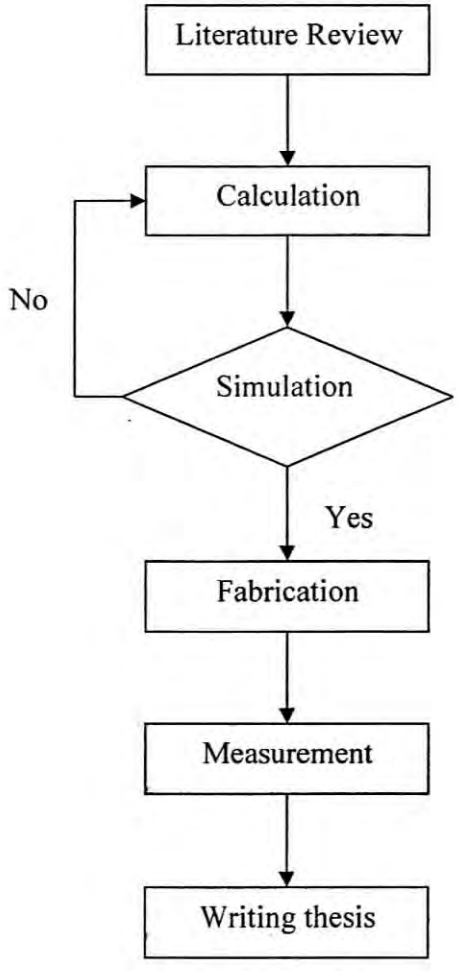

Figure 5.1: Project implementation

5.2 Microwave Office (MWO) Software

Microwave Office (MWO) enables users to design circuits composed of schematics and electromagnetic (EM) structures from an extensive electrical model database, and then generate layout representations of these designs. Users can perform simulations using one of Microwave Office's simulation engines such as a linear simulator, an advanced harmonic balance simulator, a 3D-planar EM simulator (EMSight), or an optional HSPICE simulator and display the output in a wide variety of graphical forms based on the analysis needs. Users can then tune or optimize the designs and changes are automatically and immediately reflected in the layout. In this project, circuit simulation environment have been for used to design and simulation processed. Figure 5.2 shows the general windows of MWO.

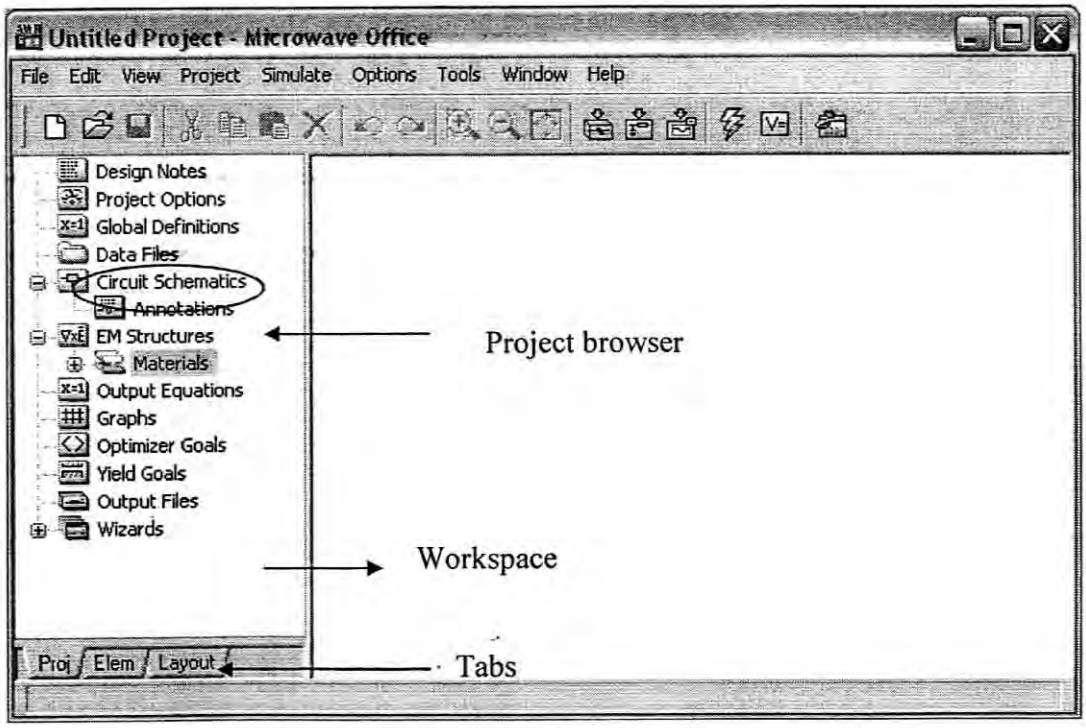

Figure 5.2: The MWO design environment

Figure 5.3 summarizes the steps that need to be followed in designing a beamforming network in Microwave Office.

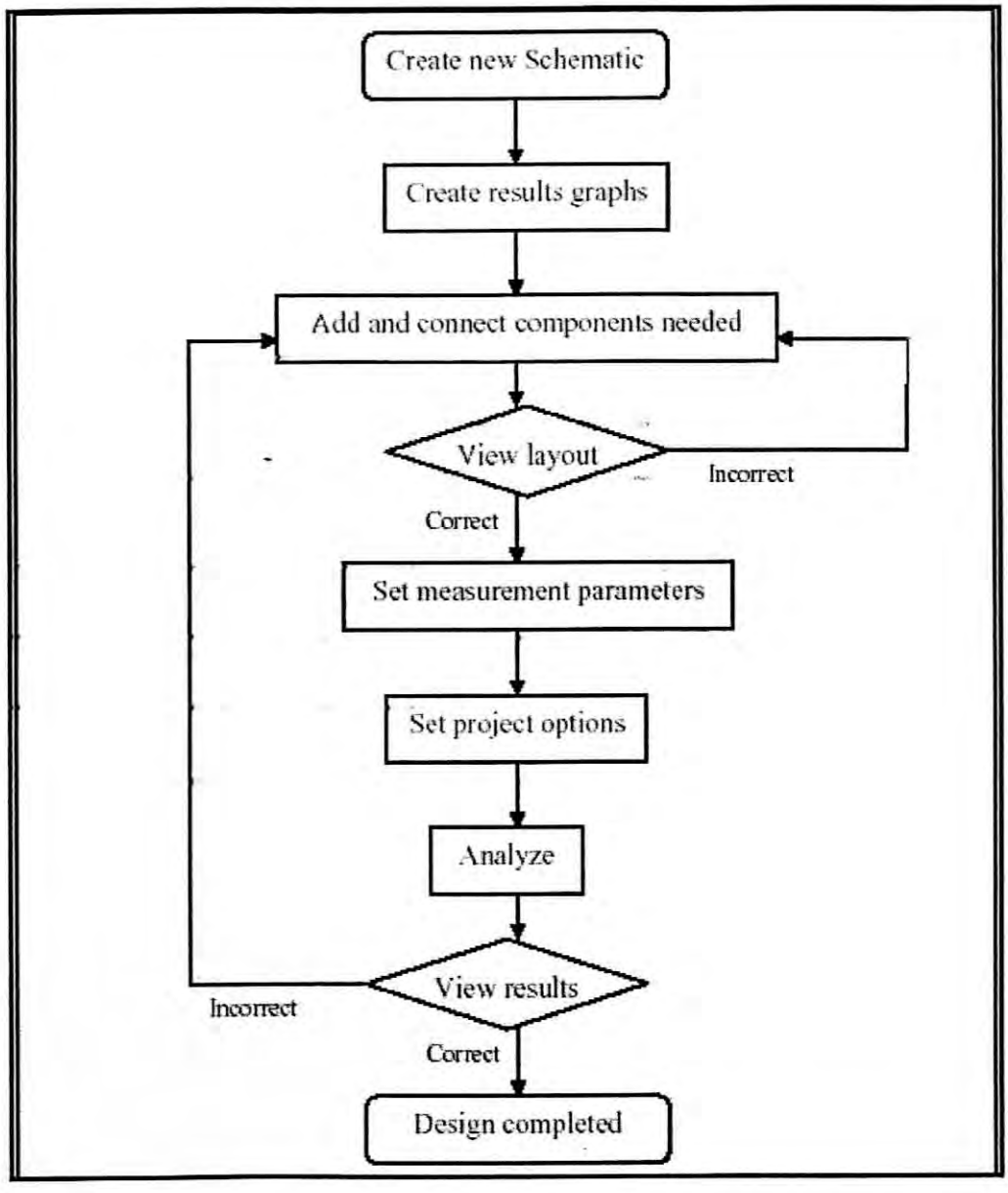

Figure 5.3: Summary of steps in using Microwave Office

6.0 DESIGN AND SIMULATION

This chapter will first explain the specifications of the material that used the general parameters and the expected results from the designs. There will be Butler Matrix design developed, that consist of will show the design of each hybrid coupler, crossover, the 4 x 4 Butler Matrix design and the simulation results.

6.1 Design Specifications and General Parameters

The material that used in this project is the FR4 PCB which has a thickness of 1.6 mm, dielectric constant of 4.7 and the dissipation factor of 0.019. The network will operate at 2.4 GHz and the characteristic impedance is 50 Ω. Using the specifications mentioned, the effective dielectric constant can be calculated using equation (1) and the wavelength, equation (2). The transmission line width and length can be calculated using equation (3) and (4).

$$\varepsilon_{eff} = \frac{\varepsilon_r + 1}{2} + \frac{\varepsilon_r - 1}{2} \frac{1}{\sqrt{1 + 12d/W}} \tag{1}$$

$$\lambda = c / f \sqrt{\varepsilon_{eff}} \tag{2}$$

$$\frac{W}{d} = \frac{2}{\pi}\left[B - 1 - \ln(2B-1) + \frac{\varepsilon_r - 1}{2\varepsilon_r}\left\{\ln(B-1) + 0.39 - \frac{0.61}{\varepsilon_r}\right\}\right] \tag{3}$$

where, $B = \dfrac{377\,\pi}{2 Z_o \sqrt{\varepsilon_r}}$

$$\ell = \frac{90°(\pi / 180°)}{\sqrt{\varepsilon_{eff}}\, k_o} \tag{4}$$

6.2 General Hybrid Coupler

Hybrid coupler is -3dB directional couplers with a 90° phase difference in the output of the through and coupled arms. These types of hybrid are often made in microstrip from as shown in Figure 4.1. The Figure 6.1 as shown the basic operation of the branch-line is as follows with all ports matched, power entering port 1 is evenly divided between port 2 and port 3, with a 90° phase shift between these outputs and no power is coupled to port 4 (the isolated port). According to the results from the earlier section together with the hybrid coupler specification, the length of the series arms are 16.65306*mm* while the length of the shunt arms are 16.266217*mm* of quarter wavelength. The width of the series arm is 4.99914*mm* while the width of the shunt arm is 2.9121378*mm*.

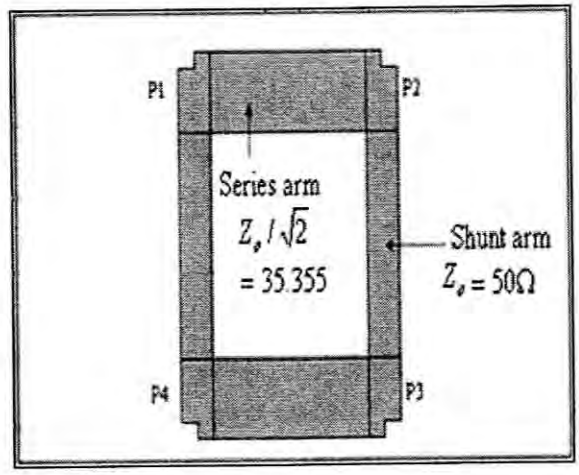

Figure 6.1: General layout of a hybrid coupler

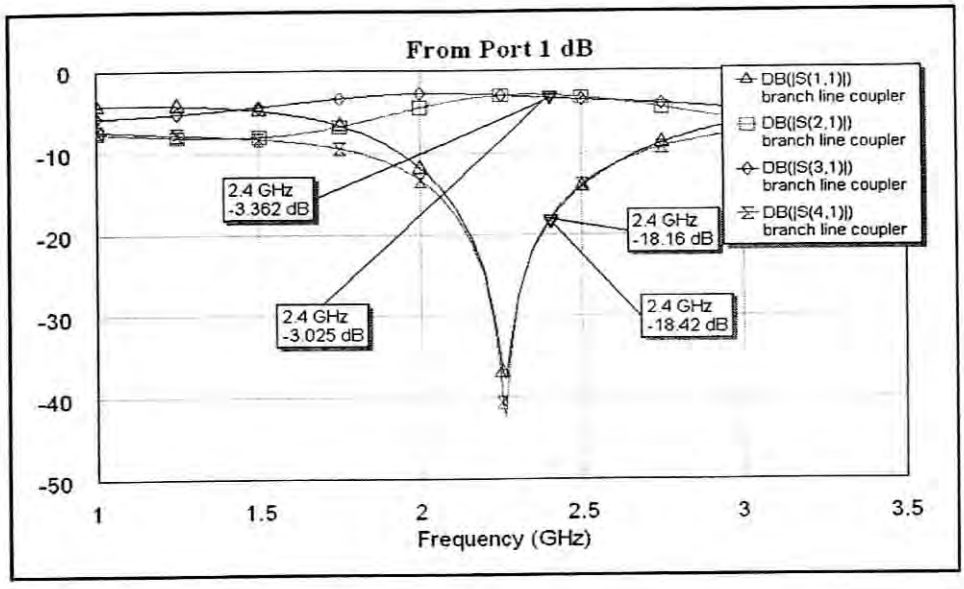

Figure 6.2: S-parameter simulation base on Port 1 in dB (Hybrid Coupler)

According to Figure 6.2, it has shown that simulation result for return loss (S_{11}), isolation (S_{41}) and coupling (S_{21} and S_{31}) in decibel (dB) value. The input from P1 to output at P1 (S_{11}) is -18.16dB while the input from P1 to output at P4 (S_{41}) is -18.42dB and compared to the value at 2.25GHz, for (S_{11}) and (S_{41}) is -37dB and -40.48dB. The value at this frequency is the accurate result compare to the value at 2.4GHz, because this value exists at needed slope (at 2.25GHz).

The simulation result for coupling at the input from P1 to output at P2 (S_{21}) is -3.025dB while at the input from P1 to output at P3 (S_{31}) is -3.362dB. Compare to the theoretical value it should be -3dB approximately to the simulation result. The result of (S_{31}) should be less than (S_{21}) because it has loss at (S_{31}). Difference among the value above occurred because the changing width and length at series and shunt arms. The purpose changing the value is to achieve 90° phase difference between at (S_{21}) and (S_{31}).

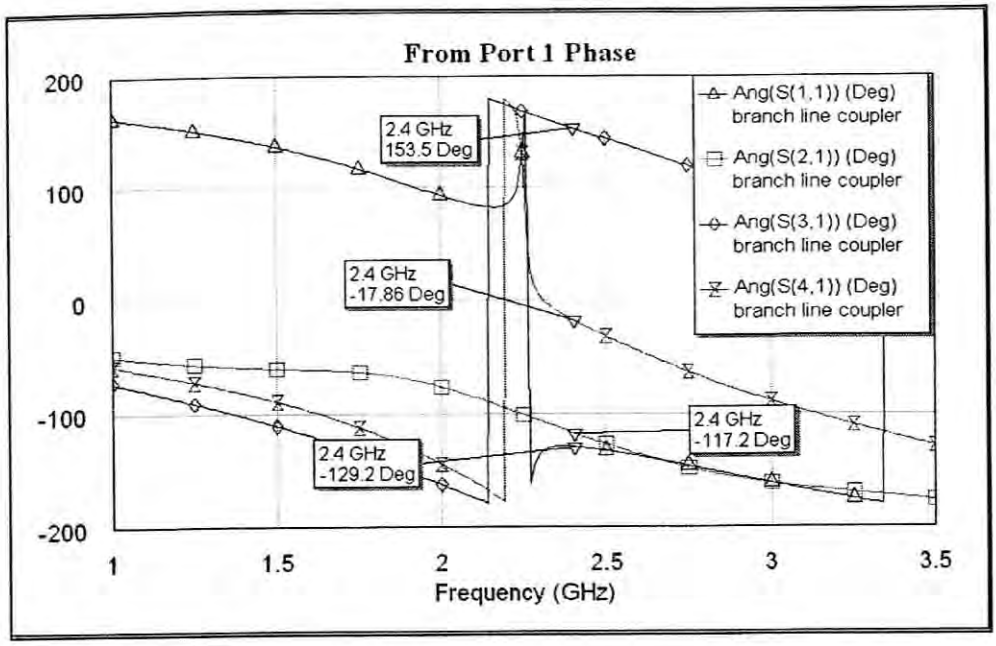

Figure 6.3: S-parameter simulation base on Port 1 in Phase (Hybrid Coupler)

The Figure 6.3 it shown that about s-parameter simulation base on P1 in phase value. The simulation result for return loss (S_{11}) is $-129.2°$ while isolation (S_{41}) result is $-17.86°$. The phase outputs from P1 varies at 2.4GHz, the phase of S_{21} is $-117.2°$ and the phase of S_{31} is $-153.5°$. The phase differences of both s-parameters are $-89.3°$, this difference is almost approximately same and very close to theoretical value, $90°$.

Table 6.1: Shows that summary of simulation result hybrid coupler

S-parameter	Parameter	Decibel (dB)	Phase
S[1,1]	Return loss	-18.16 dB	-129.2 Deg
S[2,1]	Coupling	-3.362 dB	-117.2 Deg
S[3,1]	Coupling	-3.025 dB	153.5 Deg
S[4,1]	Isolation	-18.42 dB	-17.86 Deg

6.3 General Crossover

In this project, the crossover must assure isolation between signals at the crossing of lines. Then the main role of crossover is obtained by cascading two hybrids. The general simulation of the crossover is shown in Figure 4.4.

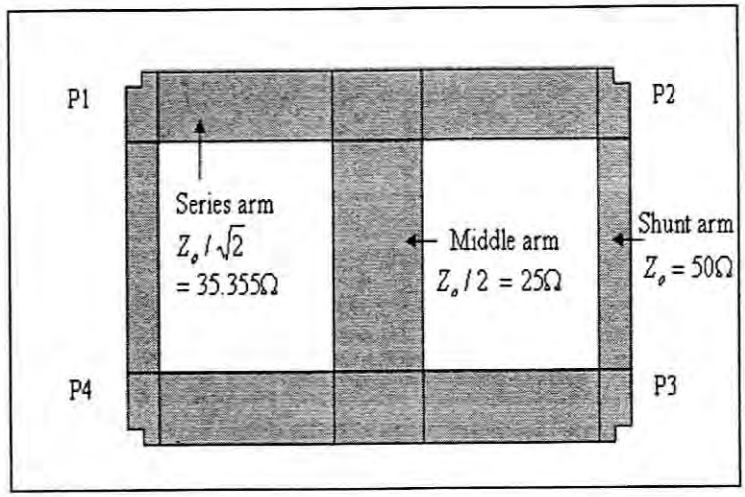

Figure 6.4: General layout of the crossover

The Figure 6.4 as shown the basic operation of the branch-line is as follows with all ports matched, power entering port 1 is evenly cross between port 1 and port 3, with a 0° phase shift between these outputs. This design at P2 can be consider as isolated from input P1 and the fraction of signal that goes to output P4 is very high. The results from the earlier section together with the crossover specification, the length of the series arms are16.65306*mm*, the length of the shunt arms are 16.266217*mm* while the middle arm is15.8621*mm*. The width of the series arm is 4.99914*mm*, the width of the shunt arm is2.9121378*mm* while the width of the middle arm is 8.19872*mm*.

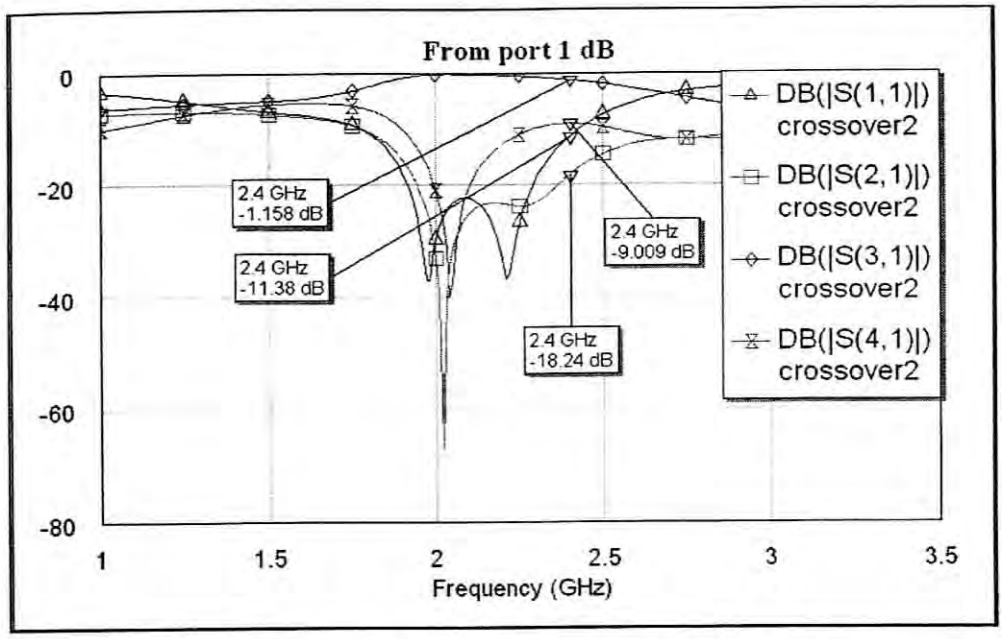

Figure 6.5: S-parameter simulation base on Port 1 in dB (Crossover)

The crossover is designed and optimized to have good return loss at acceptable level. The return loss is less than -11dB, the isolation between port 1 and 2 is -18.24dB while isolation between port 1 and port 4 (S_{41}) is –9.009dB. The simulation also show the cross line between P1 and P3 (S_{31}) is -1.158dB. The graph of s-parameter in decibel and can be seen at Figure 4.5 and s-parameter in phase as have been shown in Figure 6.6.

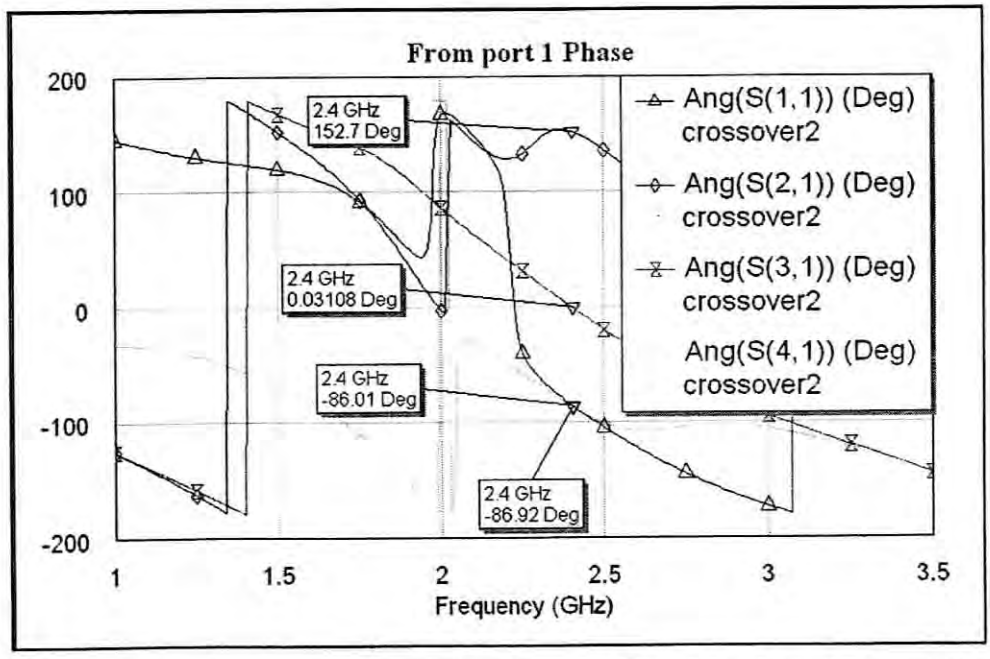

Figure 6.6: S-parameter simulation base on Port 1 in phase (Crossover)

The result at figure above as shown ate phase of S_{21} is 152.7° and the phase of S_{31} is 0.03108°. However even the phase vary with frequency, the phase at S_{31} is almost constant and very close to ideal value 0°.

Table 6.2: The summary of simulation result crossover

S-parameter	Parameter	Decibel (dB)	Phase
S[1,1]	Return loss	-11.38 dB	-86.01 Deg
S[2,1]	Isolation	-18.24 dB	-152.7 Deg
S[3,1]	Cross Line	-1.158 dB	0.03018 Deg
S[4,1]	Isolation	-9.009 dB	-86.92 Deg

6.4 Phase Shifter

After choosing hybrids coupler and crossover, this project have to find how implement phase shifter. A transmission line of length introduces phase shifter $\theta = \frac{360°}{\lambda}$ where λ is the wavelength on the substrate defined as $\lambda = \frac{c}{f\sqrt{\varepsilon_{eff}}}$, ε_{eff} is the effective permittivity of the substrate. The Figure 6.7 and 6.8, it shown the difference electrical length between that 45°,90°,180° and 360°. The result of electrical length 360° is approximate to 0° because power at input approximate with power at output.

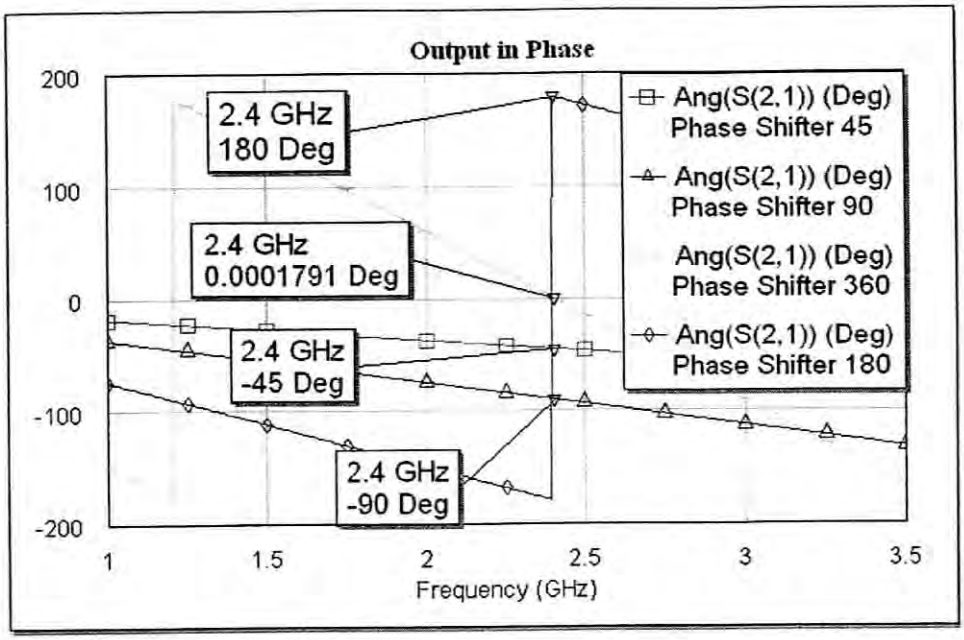

Figure 6.7: S-parameter simulation base on Port 1 in phase

6.5 Butler Matrix

The Butler Matrix consists of an equal number of input and output ports connected through an array of phase shifters and couplers such that when a signal is applied to any input port it produces equal amplitude signals at all output ports. Figure 1 shows the block diagram and Table 1 shows the specification of the 4x4 Butler Matrix.

In this project, the circular and mitered bend designs for the beamforming network are developed. The transmission lines in circular bend has been placed far from each other while for mitered bend, it is placed closely. This is to determine the coupling effect of transmission line proximity. The output ports for circular bend have been spaced in such a way that antennas can be attached directly to the network. The output ports for circular bend have been spaced in such a way that antennas can be attached directly to the network. Four hybrid couplers and a crossover were combined to produce a Butler Matrix. The design specifications for the Butler matrix for magnitude are shown in Table 6.3 and Table 6.4 shows the design specification for phase.

Table 6.3: Design specifications (magnitude) of the Butler Matrix

S- Parameter	Parameter	Specification
S[1,1]	Return loss	≤-14 dB
S[2,1]	Isolation	≤-14 dB
S[3,1]	Isolation	≤-14 dB
S[4,1]	Isolation	≤-14 dB
S[5,1]	Coupling	-6.45 +/- 0.25 dB
S[6,1]	Coupling	-6.45 +/- 0.25 dB
S[7,1]	Coupling	-6.45 +/- 0.25 dB
S[8,1]	Coupling	-6.45 +/- 0.25 dB

Table 6.4: Design specifications (phase) of the Butler Matrix

Ports	A1	A2	A3	A4	β
1R	0°	– 45 °	– 90 °	135 °	45 °
2L	– 90 °	45 °	180 °	– 45 °	– 135 °
2R	– 45 °	180 °	45 °	– 90 °	135 °
1L	– 135 °	– 90 °	– 45 °	0°	– 45 °

6.5.1 Circular Bend

Four hybrid couplers, two crossovers and phase shifters were combined to obtain the Butler Matrix in circular bend shown in Figure 6.8. The size of the layout is 207.52mm mm in length and 88.16mm in width. The 45 degree phase shifter, together with phase adjustment, is obtained by connecting a transmission line at an output port of a hybrid coupler to at an input port of the other. At the output ports, additional transmission lines is placed at space the ports in such a way that antenna can be directly connected to the network.

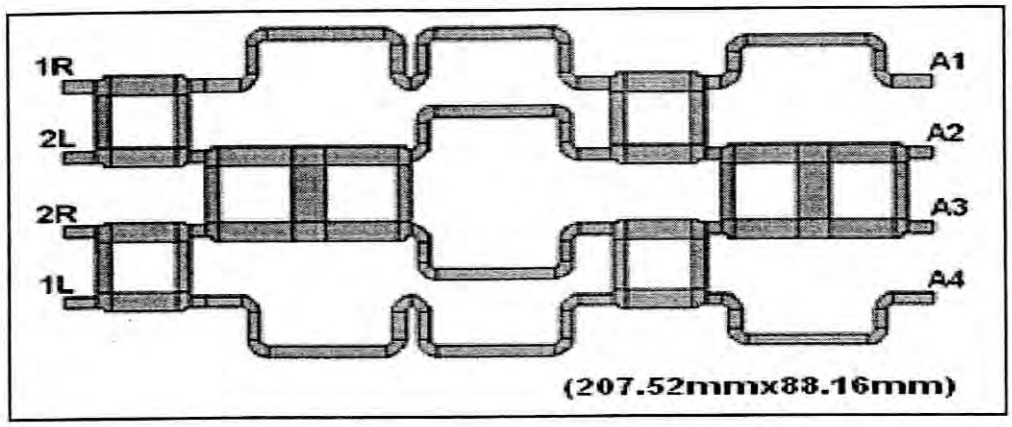

Figure 6.8: Butler Matrix layout for circular bend

Figure 6.9 shows the return loss and isolations at the input ports are below -19.82dB. Figure 6.10 shows the output ports which are around -6 to -10 dB. The output phase difference (β) is shown in Figure 6.11. β is the phase difference of excitation current between output ports provided by the Butler Matrix. Table 6.5 summarizes the simulation results for return loss, isolation in magnitude (dB) and Table 6.6 summarizes of magnitude and phase results for simulation result.

Table 6.5: Return loss and isolation in magnitude (dB)

S-Parameter	Parameter	Magnitude (dB)
S[1,1]	Return Loss	-11.4
S[2,1]	Isolation	-18.29
S[3,1]	Isolation	-19.82
S[4,1]	Isolation	-14.97

Table 6.6: Summary of magnitude and phase results for simulation result

	Ports	A1	A2	A3	A4	β
Mag (dB)	R1	-7.45	-9.66	-10.8	-9.61	-
Phase (°)		5.06	-42.1	-84.7	-143	49.35
Mag (dB)	L2	-10.3	-8.82	-7.52	-9.93	-
Phase (°)		-87.2	44.08	-178	-45.8	-133
Mag (dB)	R2	-8.82	-7.52	-9.93	-10.3	-
Phase (°)		-45.8	-178	44.08	87.2	133
Mag (dB)	L1	-9.61	-10.8	-9.66	-7.45	-
Phase (°)		-143	-84.7	-42.6	5.06	-49.35

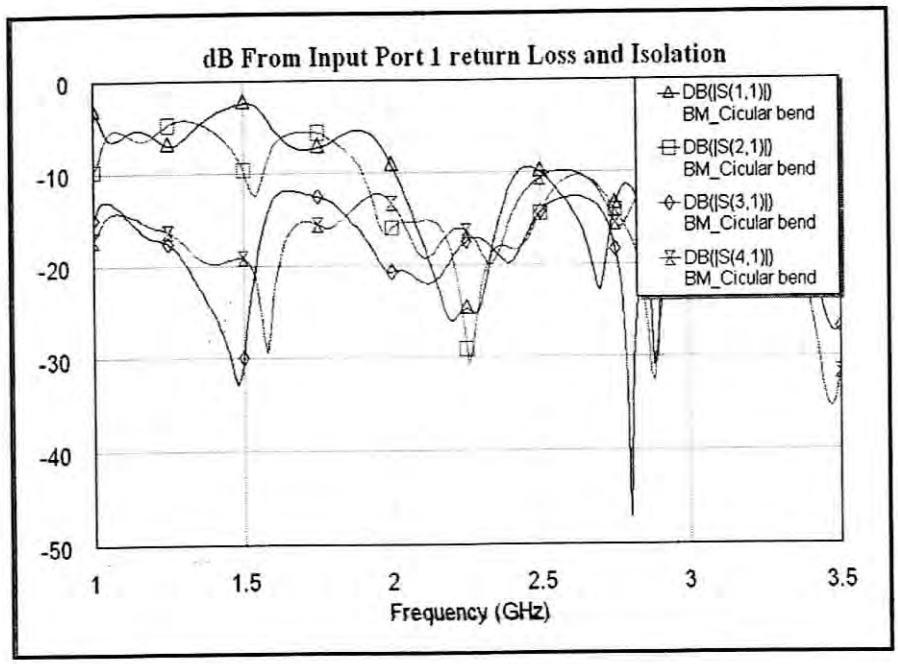

Figure 6.9: S-parameter simulation results for the return loss and isolations

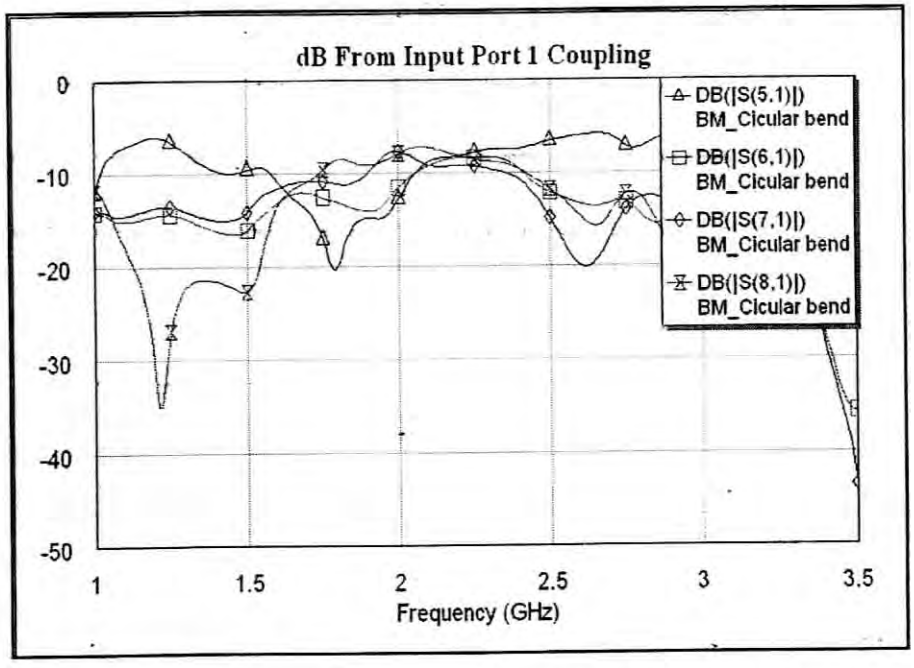

Figure 6.10: S-parameter simulation results for the coupling coefficient

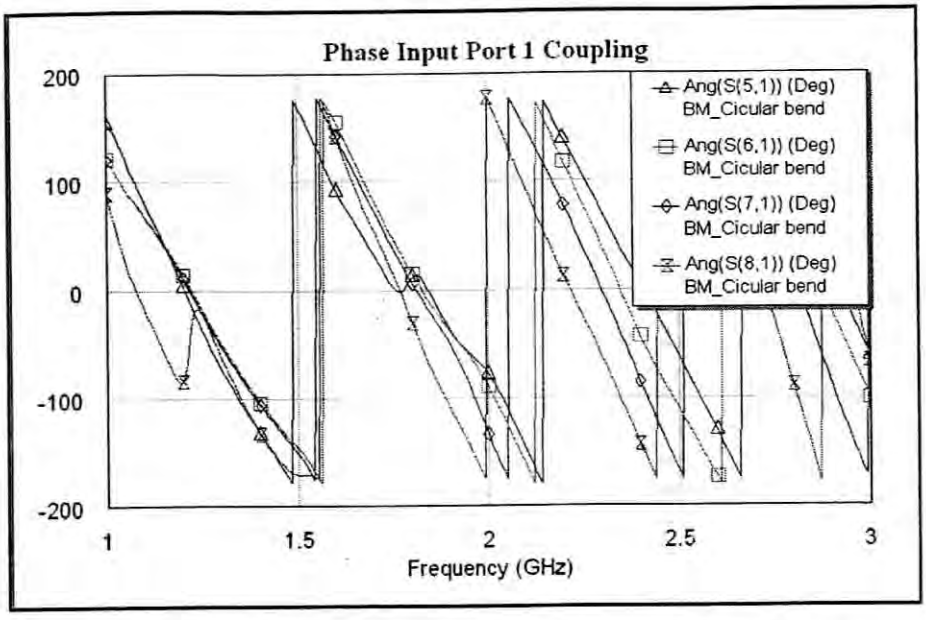

Figure 6.11: S-parameter simulation results for the output phase difference (β)

6.5.2 Mitered Bend

The second design is a compact layout using mitered bend. The advantage of using Butler Matrix is that it gives freedom to the designer to place the components according to his creativity to optimize space. The size of the layout is 191 mm in length and 70.9 mm in width. Mitered bends are space efficient, therefore it is possible to obtain a compact design.

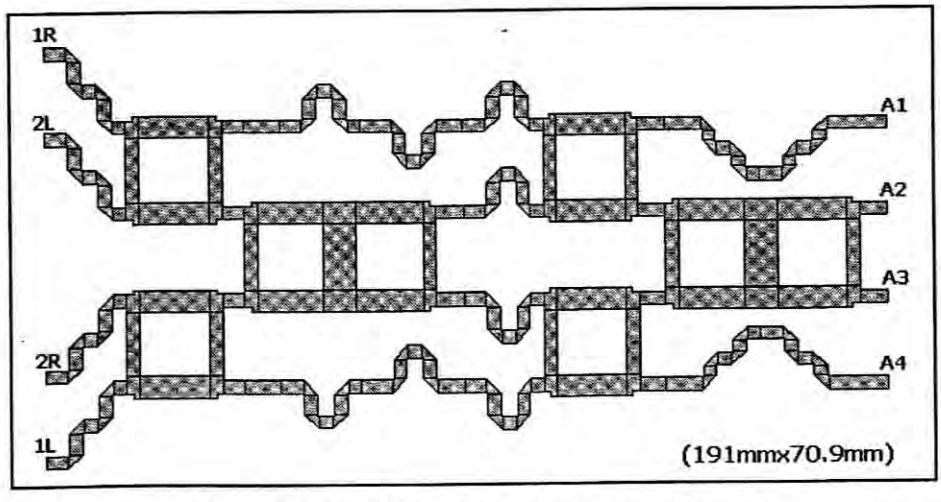

Figure 6.12: Butler Matrix layout for mitered bend

The simulation of Butler matrix by using mitered bend has been done. It can be seen clearly that using rounded bend is not space efficient compared to using straight line. However it must be noted that design is able to accommodate the array of antennas directly to its output ports. Figure 6.13 shows the return loss and isolations at the input ports are below -22.67 dB. Figure 6.14 shows the output ports which are around -7.4 to -10.9 dB. The output phase difference is shown in Figure 6.15. The simulation results in return loss, isolation and coupling are summarized into Table 6.7 and 6.8.

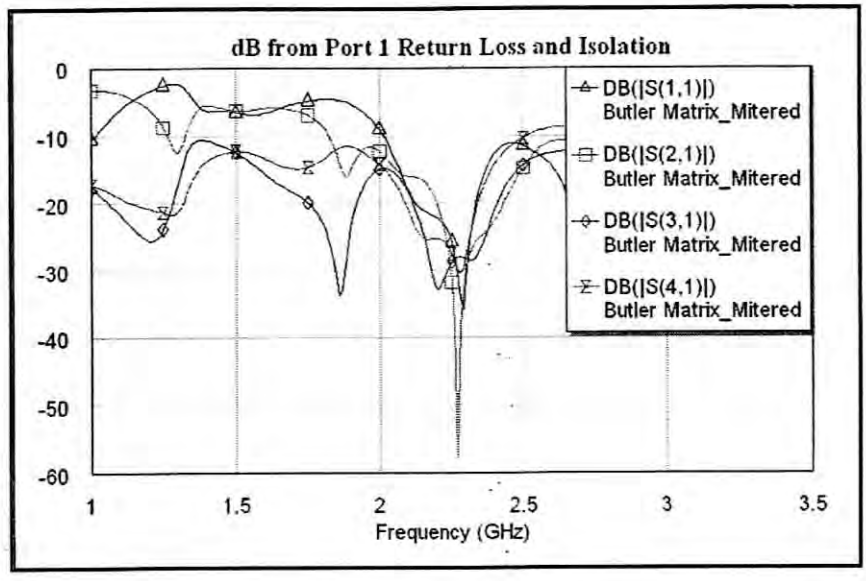

Figure 6.13: S-parameter simulation results for the return loss and isolations

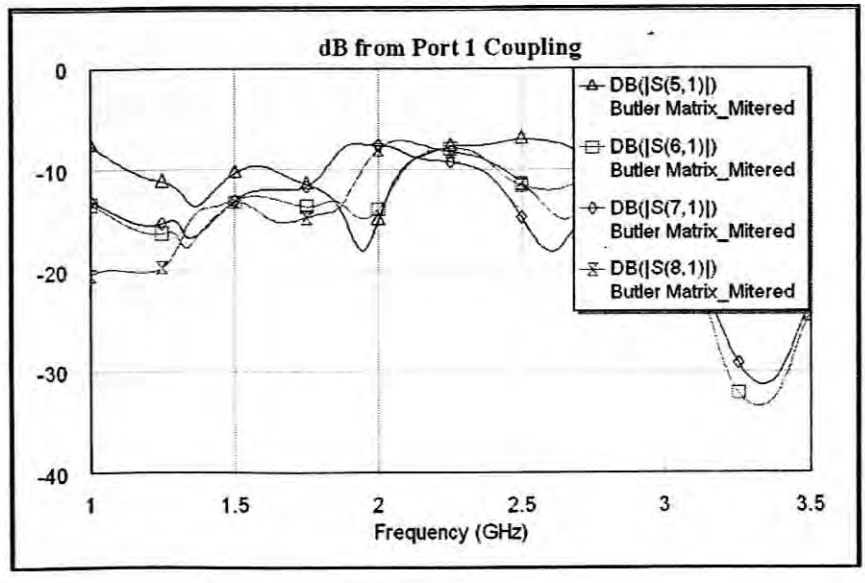

Figure 6.14: S-parameter simulation results for the coupling coefficient

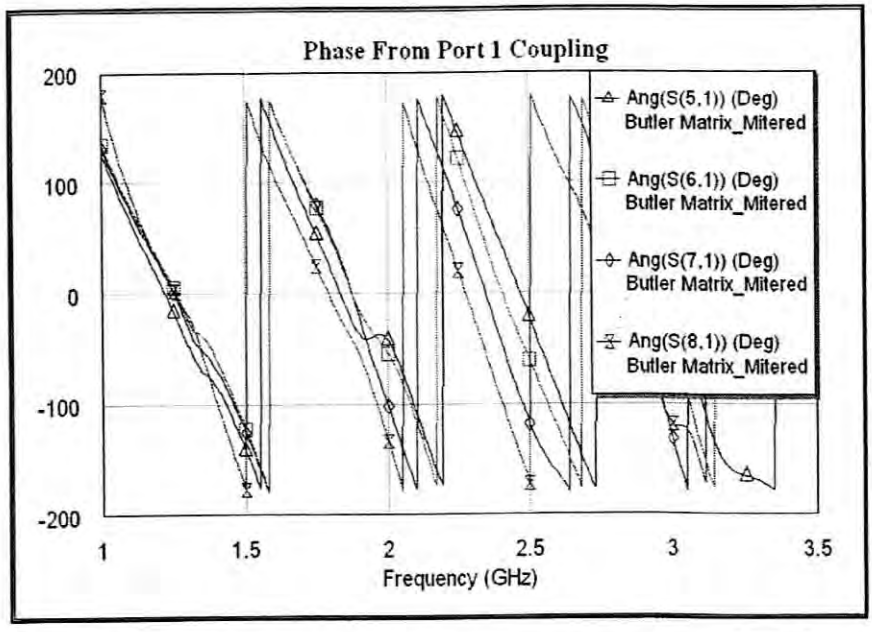

Figure 15: S-parameter simulation base on Port 1 shows the output phase difference

Table 6.7: Summary of coupling coefficient for simulation result

S-Parameter	Parameter	Magnitude (dB)
S[1,1]	Return Loss	-12.63
S[2,1]	Isolation	-22.67
S[3,1]	Isolation	-21.05
S[4,1]	Isolation	-14.21

Table 6.8: Summary of magnitude (dB) and phase for simulation result

	Ports	A1	A2	A3	A4	β
Mag (dB)	R1	-7.43	-9.62	-10.94	-9.41	-
Phase (°)		45.1	2.82	-43.86	-97.1	47.38
Mag (dB)	L2	-9.17	-8.87	-7.84	-9.21	-
Phase (°)		-42.4	87.04	-140	-1.54	-134.83
Mag (dB)	R2	-8.87	-7.84	-9.21	-9.17	-
Phase (°)		-1.71	-140	86.86	-42.39	134.83
Mag (dB)	L1	-9.41	-10.94	-9.62	-7.43	-
Phase (°)		-97.1	-43.86	2.82	45.1	-47.38

6.6 Simulation Results Analysis

The overall result, the ports are noted horizontally and vertically as any ports can be the input while the other ports in the respective column or row would be the output. These are due to the high degree symmetry of the design besides the results obtained before and after inverting the input and output ports are identical. Problem however arises in obtaining good isolation and couplings. This has been solved by cascading two hybrid couplers for crossover and adjusting the length and width of transmission lines.

There is a slight difference in the crossover results between the two designs. The return loss and isolations for circular bend are slightly better than mitered bend. However, the coupling for mitered bend is better than circular bend. The coupling requirements do not meet the exact requirements but other parameters do. Both designs show small error in phase output. The crossovers designed are therefore good isolators at the crossing of transmission lines. The both designs exhibit similar results in return loss and isolations. The results for these parameters are better than the design specifications. However mitered bend has better coupling than circular bend of about 4 dB. Though mitered bend has better coupling, both designs are still not able to meet the requirements. The output phases for both designs generally display small errors, with the maximum and minimum for circular bend being 2 and 4.35 respectively, while for mitered bend, it is 0.17 and 2.38.

Simulation results were also seen when the input and output ports were inverted. From the results obtained for both designs, it can be concluded that the both Butler Matrix have a high degree of symmetry. This is because the results obtained before and after inverting the ports are identical. Since narrowband hybrid couplers and crossovers have been used in this project, the bandwidth in which the Butler matrix may operate well is relatively small. The bandwidth here is determined by looking at the difference between the return loss and isolations and coupling magnitudes.

7.0 FABRICATION AND MEASUREMENT

In this chapter, the fabrication method employed for both designs are first explained. This is followed by the equipment used to test the parameters and the methods to obtain results. The results of the fabrication will then be shown and analyzed.

7.1 Fabrication Method

Before beginning the fabrication process, the layout would have to be prepared by printing it with its exact dimensions on a transparency. This is done using the CorelDRAW software. The layout has to be printed using a laser jet printer to ensure the printing quality is at its best. However if the quality is not satisfactory, the layout has to be darkened further using a transparency marker.

After the layout has been well prepared, the transparency is placed together with a new FR4 photo board into the UV light equipment. This equipment is shown in Figure 7.1. The function of the UV equipment is to impose the layout upon the photo board. When the imposing process is completed, the photo board is placed on a fabrication tray. To make the layout visible, the developer chemical is poured into the tray. After several minutes of moving the tray from side to side to hasten the developing process, the layout would be visible.

The process is continued by taking the board out of the first tray and placing it into a second tray filled with water. Ferrite chloride acid is used to etch the layout. The acid will be poured into another tray until it submerges the board. The etching process is done by moving the tray from side to side.

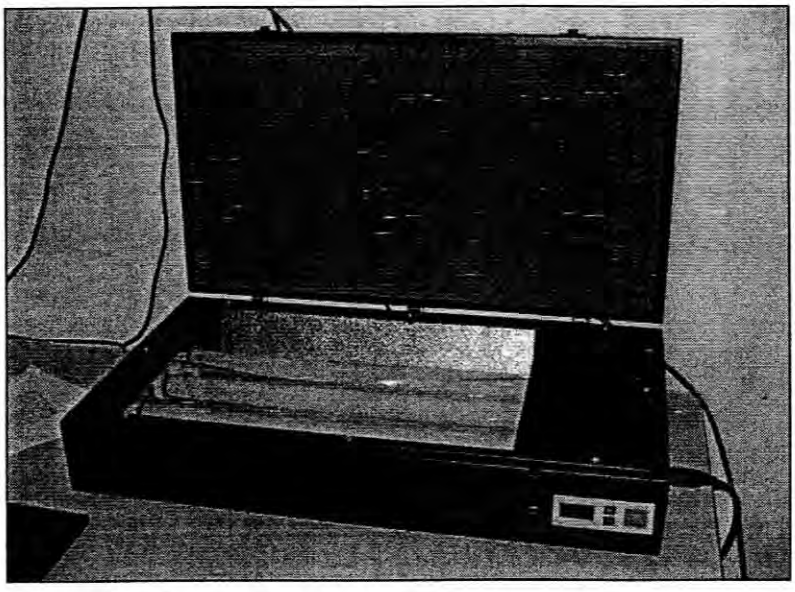

Figure 7.1: The UV equipment

Each design typically takes three hours to complete the etching process. When the etching process has been completed, the FR4 board is washed with water. If there are acid residuals visible, they are removed using the stain remover. The fabrication process will be completed by gently wiping the board with thinner. Finally, connectors are soldered at the ports to enable measurement. The designs that were fabricated are shown in Figure 7.2 (circular bend) and Figure 7.3 (mitered bend).

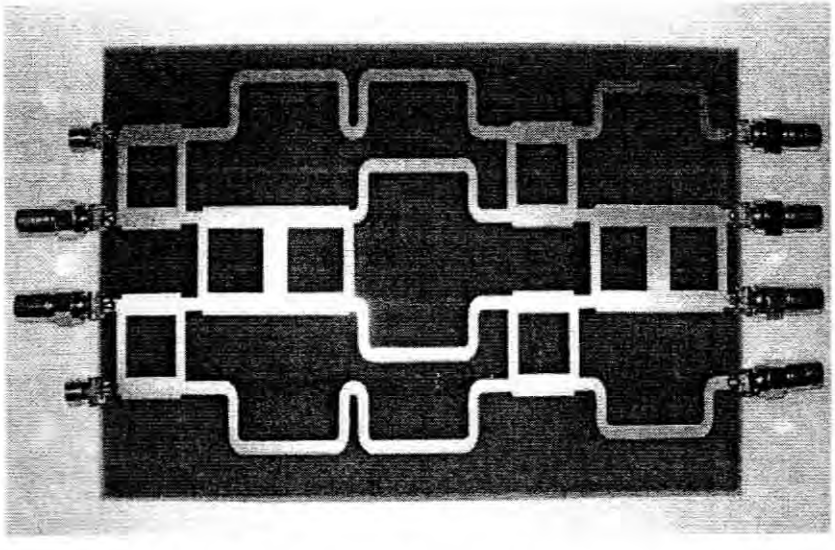

Figure 7.2: Fabrication of Butler Matrix (Circular Bend)

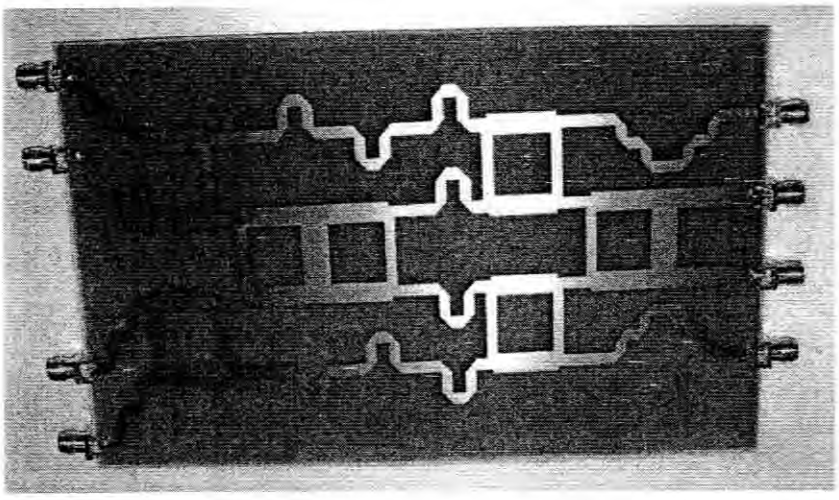

Figure 7.3: Fabrication of Butler Matrix (Mitered Bend)

Each connector is priced at approximately RM 23. The total cost of the connectors would be RM 368 since 16 connectors would be required (eight for each design). The FR4 photo board that has been used for both designs are estimated to have cost RM 100. Therefore the cost estimation for my project fabrication, including the cost of the other materials used, would be approximately RM 500. Total costs have been borne by the PSM LAB.

7.2 Measurement Methods

Three parameters were successfully tested using the equipments at the Telecommunication Lab. The parameters are the return loss, isolation and coupling and the phase output was able to be tested as the Advantest R3767 Network Analyzer. This equipment is shown in Figure 7.4. A cable would be connected to the port at which the return loss, isolation and transmission line is measured while the other ports are terminated with matched loads.

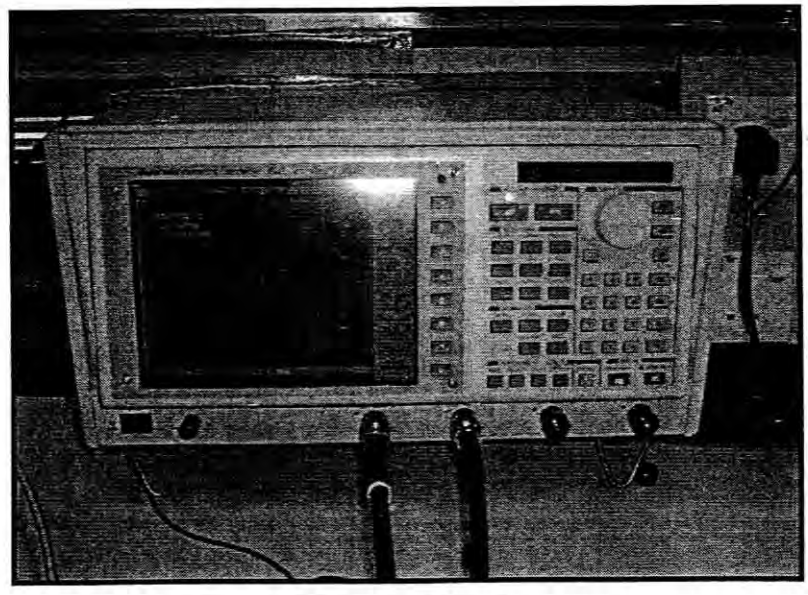

Figure 7.4: The Network Analyzer

The measuring for these parameters, the first cable is connected to the input port cable at one end while the other end is connected to the output port cable. The other ports are terminated with matched loads as shown in Figure 7.6.

Figure 7.6: Picture shows the isolation being measured at Port 1 while all other ports are terminated with matched loads.

7.3 Measurement Results

The fabrication of Butler Matrix has been done and the measurement result has phase error compared to simulation result. Only one port is activated at one time, other ports are terminated with 50 ohm terminator while all input ports are fed with same signal. With reference to the fabrication design, both designs exhibit some error results in return loss and isolations. The simulation result has better transmission coefficient than fabrication result. The output phases for both designs generally display some errors. As mentioned before, the variation of the values may be due to the physical loss factor that the butler matrix also provides constant phase increment between output ports.

Table 7.1: Comparison of return loss and isolation in magnitude (dB) for both design

S-Parameter	Parameter	Magnitude (dB)	
		Circular	Mitered
S[1,1]	Return Loss	-18.72	-16.22
S[2,1]	Isolation	-34.64	-22.59
S[3,1]	Isolation	-28.41	-32.48
S[4,1]	Isolation	-20.15	-17.85

The circular design, it can be seen that the return loss result for fabrication and simulation have some difference values. These results which are in the highest return losses for fabrication occurred around 2.52GHz. All the return losses at 2.4 GHz are below -18.72dB, which fulfills the design specifications. However, not all the isolation fulfills the requirements that have been set earlier. The values are around -20.15 to -34.64dB. The couplings exhibit better results than the design requirements and simulation results. The measurement values range from -8.92 to -12.32dB.

Table 7.2: Comparison of coupling in magnitude (dB) for measurement result

S-Parameter	Parameter	Magnitude (dB)	
		Circular	Mitered
S[5,1]	Coupling	-8.92	-9.12
S[6,1]	Coupling	-10.08	-9.31
S[7,1]	Coupling	-12.32	-9.81
S[8,1]	Coupling	-11.29	-12.06

The return loss graphs for mitered bend shows some difference values between the simulation and measurement results. The graphs are almost identical with the return losses at 2.4 GHz all below -17dB, which fulfills design specifications. The good results in the highest return losses for fabrication occurred around 2.49GHz. The isolations values at 2.4 GHz on the other hand display a range of values from -17.85 to -32.48dB. Therefore not all isolations meet the requirements. The coupling values, as in circular design, exhibit not a better result than the simulation results and design requirements. The values are at 2.4 GHz range from -9.12 to -12.06dB.

Table 7.3: Comparison of coupling in phase difference (β) for measurement result

Phase (°)	Ports	A1	A2	A3	A4	β
Circular	R1	121.32	75.41	49.60	-29.61	50.31
Mitered		96.16	36.25	-11.07	-41.88	46.01
Circular	2L	43.27	146.71	-65.6	75.51	-130.74
Mitered		-15.42	101.93	-113.19	42.22	-139.21
Circular	R2	74.46	-70.61	149.16	34.51	133.32
Mitered		27.41	-114.63	99.48	-12.83	133.41
Circular	L1	-33.82	47.12	65.92	114.41	-26.86
Mitered		-61.18	6.79	24.51	89.85	-50.34

It must be noted that in circular design, transmission lines have been spaced as far as possible from each other, while in mitered bend, they have been placed closely. The reason for this technique is to check for coupling effects due to the proximity of the transmission lines. This effect is not able to be taken into account by the Microwave Office Schematic simulations.

However in the measurement results, obviously the proximity of the transmission lines does not exhibit much difference of the results between the two designs. From the analysis, it is clear that mitered bend performs better than circular design at 2.4 GHz. The return loss and coupling coefficient are better than circular design while the isolation value varies.

Both designs are expected to show difference (β) since there is a significant difference at the coupling coefficient, return loss and isolation values. The values may not match the simulation results but mitered bend is expected to display a more constant phase difference between the outputs results compared to circular design. The return loss was measured at all ports of the prototype to prove that the fabricated design has a high degree of symmetry as well. Fabrication process on an actual FR4 PCB may not contribute the exact results as seen in the simulation as the method used will be basic and is prone to resulting in non-uniformity of the transmission line width.

The phase errors seen in a fabricated network would probably be higher. It is also important to note the placing of the pins that would be the input and output ports on the fabrication. This would show the different of transmission line length when compared with the simulation done. There seem to be significant differences in the simulation and measurement values especially for circular design. The possible reasons that could attributed to this fact is the basic fabrication process employed, the non-uniformity of transmission line width in the fabrication, the difference in length is created when the connectors are soldered and the possibility that there may have been errors during the measurement process.

8.0 CONCLUSION

In this project, a 4x4 Butler Matrix has been calculated, designed and simulated at 2.4GHz band. The circuit is compact and has low losses. In the proposed design, the hybrid coupler, crossover and phase shifter were also designed, simulated and fabricated. Calculation and simulation of magnitude show a good agreement. The proposed system has the advantages of low cost, small volume, light weight and ease of fabrication later. All components (a hybrid junction, phase shifter, and crossover) are developed in this technique.

The phase shift is realized by a path difference. Thus, it is linearly frequency dependent. The most critical component is the cross since it can cause significant amplitude and phase errors. The proposed Butler Matrix is suitable for wireless applications such as IEEE802.11n technology.

8.1 Suggestion

The Butler Matrix will be accomplished with compact size. This is necessary for implementation in the wireless access point and possibly the mobile unit. The constrains of meandering lines in microstrip will quickly be breached. One means of truncating the size of this design will be use of ferroelectronic thin film. These materials have much higher dielectric constants and are thus inherently smaller. In addition the use of embedded passive to serve as the hybrid couplers will continue to push this device closer to commercially viability.

REFERENCES

[1] M.Bona, "Low loss Butler matrix for a microstrip," M.S. thesis, KTH Royal Inst, Technol, Stockholm, Sweden, 2000.

[2] Ng Chee Tiong Desmond, Smart Antennas for Wireless Applications and SwitchedBeamforming, Department of Information Technology and Electrical Engineering the University of Queensland, 2001.

[3] Tayeb A. Denidni and Taro Eric Liber "Wide Band Four-Port Butler Matrix for Switched Multibeam Antenna Arrays" IEEE, vol. 14, pp. 2461-2464, 2003.

[4] A. F. Molisch, M. Z. Win and J. H. Winters, "Capacity of MIMO Systems with Antenna Selection", in *Proc. IEEE Intl. Contr. Conf.*, Helsinki, Finland, 2001, pp. 570-574.

[5] J. Butler and R. Lowe, "Beam-Forming Matrix Simplifies Design of Electronically Scanned Antennas," Electronic Design, pp. 170-173, April 12, 1998.

[6] Kai Dietze, Carl Dietrich, and Warren Stutzman, Vector Multipath Propagation Simulator (VMPS), Draft report, Virginia Tech Antenna Group, April 7, 1999.

[7] Frank Caldwell Jr., J. Stevenson Kenney, Mary Ann Ingram "'.Design and Implementation ofa Switched-Beam Smart Antenna for an 802.11b Wireless Access Point" , IEEE Antennas and Propagation Magazine, 2002.

[8] Hitoshi Hayashi, Donald A. Hitko, Charles G. Sodini "Four Element Planar Butler Matrix Using Half- Wavelength Open Stubs", IEEE Microwave and Wireless Components Letters , March 2002 , Vol. 12, No. 3:pages 73-75.

[9] J. Litva and T. K.-Y. Lo, Digital Beamforming in Wireless Communications, Artech House, Boston, 1996.

[10] J. R. Treichler and B. Agee, A New Approach to Multipath Correction of Constant Modulus Signals," IEEE Trans. Acoustic, Speech, and Signal Processing, vol. ASSP-31, pp. 459-472, Apr. 1983

[11] Frank Caldwell Jr., J. Stevenson Kenney, Mary Ann Ingram "Design and Implementation ofa Switched-Beam Smart Antenna for an 802.11b Wireless Access Point" , IEEE Antennas and Propagation Magazine, 2002.

[12] David M. Pozar, "Microwave Engineering", John Wiley & Sons Inc.,2005.

[13] Angelucci, A., and Borocco, R. , "Optimised synthesis of microstrip branch-line couplers taking dispersion, attenuation loss & T-junction into account" , Microwave Symposium Digest , 1998 , IEEE MTT-S International. 25-27 May 1988: pages 543-546.

[14] Ahmed EL Zooghby , "Potentials of Smart Antennas In CDMA Systems and Uplink Improvements", IEEE Antennas and Propagation Magazine, October 2001, Vol. 43, No. 5.

[15] J. Butler, R. Lowe. Beamforming matrix simplified design of electronically scanned antennas. *Electronic Design.* 1961. Volume 9: pages 170-173.

[16] Stefano Mosca, Filiberto Bilotti, Allesandro Toscano, Lucio Vegni. A Novel Design Method for Blass Matrix Beam-Forming Networks. *IEEE Transactions on Antenna and Propagation.* February 2002. Volume 50: no. 2.

[17] Moody, H. J.. The Systematic Design of the Butler Matrix. *IEEE Transactions on Antenna and Propagation.* 1964. Volume 2: pages 786-788.

[18] Bachman, H. L.. *Smart antennas-the practical realities*. Proceeding IEEE Aerospace Conference, New York, NY, USA. 1997: pages 60-70.

[19] Alexander Kuchar, Michael Tangemann, Ernst Bonek. A Real-Time DOA-Based Smart Antenna Processor. *IEEE Transactions on Vehicular Technology*. 2002. Volume 51: no. 6.

[20] S. Egami, M. Kawai. An Adaptive Multiple Beam System Concept. *IEEE Journal on Selected Areas in Communications*. May 1987. Volume SAC-5: pages 630-636.

[21] Wei-Ren Dong, A. Roederer. *Analysis of Antenna Multiport Beam Forming Networks by Matrix Operation.* Proceeding ESA Workshop on Antenna Technologies. Nordwijk, The Netherlands. November 1989.

[22] R. W. Burns, R. L. Holden, R. Tang. Low cost Design Techniques for Semiconductor Phase Shifter. *IEEE Transaction on MTT*. June 1974. Volume 22: pages 675-688.

[23] Angelucci, A, Audagnotto, P., Corda, P., Piovano, B.. *Multiport Power Amplifiers for Mobile-radio Systems using Microstrip Butler Matrices.* Proceeding IEEE AP-S. Seattle, United States. 1994.

[24] Tayeb A. Denidni, Taro Eric Libar. *Planar Feeding Network for a Switched Beam Antenna Array*. ISMOT Proceedings. June 2001.

[25] J. Paul Shelton, James K. Hsiao. Reflective Butler Matrices. *IEEE Transactions on Antennas and Propagation*. September 1979. Volume AP-27.

[26] Zhenghe Feng, Yu Yang. *Multibeam plane array using modified Butler Matrix circuits*. Microwave Conference, Asia Pacific. 1991. Volume 1: pages 103-106.

[27] Lee, W. C. Y.. *An Optimum Solution of the Switching Beam Antenna System.* Vehicular Technology Conference. 1997. Volume 1: pages 170-172.

[28] K. H. Li, M. A. Ingram, E. O. Rausch. Multibeam Antennas for Indoor Wireless Communications. *IEEE Transactions on Communications*. February 2002. Volume 50, no. 2: pages 192-194.

[29] J. H. Winters, J. Salz, R. D. Gatlin. The Impact of Antenna Diversity on the Capacity of Wireless Communication System. *IEEE Transactions on Communications*. February 1994. Volume 42, no. 2: pages 1740-1751.

[30] J. R. James, P. S. Hall, C. Wood. *Microstrip Antenna Theory and Design.* Northampton, UK: A. Wheaton & Co.. 1981.

[31] Ramesh Garg, Prakash Bhartia, Inder Bahl, Appisak Ittipiboon. *Microstrip Antenna Design Handbook.* Norwood, MA: Artech House Inc.. 2001.

[32] Stephen A. Maas. Nonlinear Microwave Circuits. Norwood, MA: Artech House Inc.. 1998.

[33] George D. Vendelin, Anthony M. Pavio, Ulrich L. Rohde. Microwave Circuit Design Using Linear and Nonlinear Techniques. New York, NY: John Wiley & Sons Inc..1990.

APPENDIX A
CALCULATION AND SIMULATION OF HYBRID COUPLER

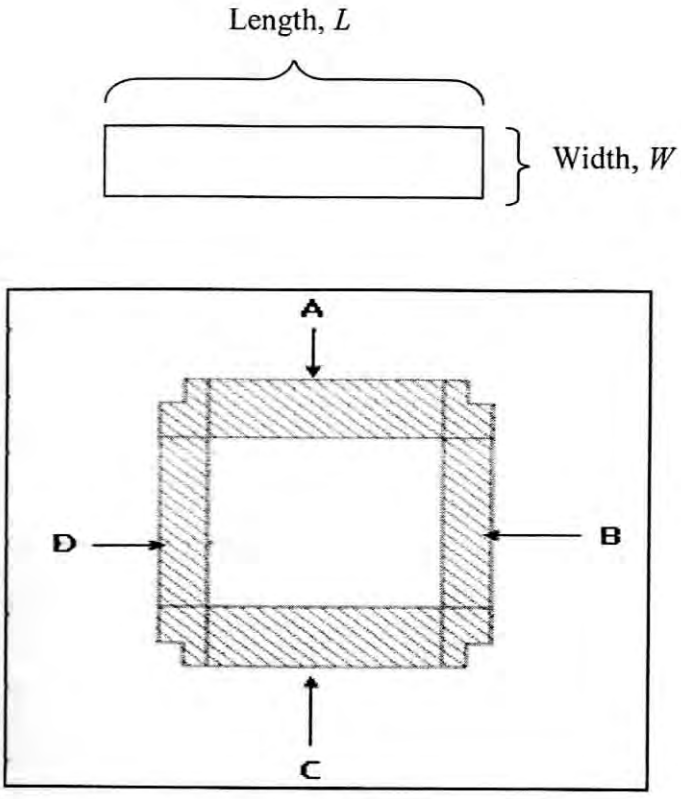

Figure A.1: General layout of a hybrid coupler

Frequency = 2.4GHz and Height (d) = 1.6mm

Section A (For A, C)

$$\frac{Z_o}{\sqrt{2}} = \frac{50}{\sqrt{2}}$$

$$= 35.3553\Omega$$

$$B = \frac{377\pi}{2Z_o\sqrt{\varepsilon_r}} \tag{4.3}$$

$$= \frac{377\pi}{2x35.3553\sqrt{4.7}} = 7.72605$$

$$\frac{W}{d} = \frac{2}{\pi}\left[B - 1 - \ln(2B-1) + \frac{\varepsilon_r - 1}{2\varepsilon_r}\left\{\ln(B-1) + 0.39 - \frac{0.61}{\varepsilon_r}\right\}\right] \tag{4.2}$$

$$= \frac{2}{\pi}\left[7.72605 - 1 - \ln(2x7.72605 - 1) + \frac{4.7-1}{2(4.7)}\left\{\ln(7.72605 - 1) + 0.39 - \frac{0.61}{4.7}\right\}\right]$$

$$= 3.124466mm$$

$$W = 3.124466x1.6mm \ = 4.99914mm$$

$$\varepsilon_{eff} = \frac{\varepsilon_r + 1}{2} + \frac{\varepsilon_r - 1}{4\sqrt{1 + \frac{12d}{w}}} \tag{4.1}$$

$$= \frac{4.7+1}{2} + \frac{4.7-1}{4\sqrt{1 + \frac{12(1.6mm)}{4.99914mm}}} = 3.69085$$

$$k_o = \frac{2\pi f}{c} = \frac{2\pi(2.4GHz)}{3x10^8} \tag{4.6}$$

$$= 50.2655m^{-1}$$

$$\ell = \frac{90°(\pi/180°)}{\sqrt{\varepsilon_{eff}}k_o} = \frac{90°(\pi/180°)}{\sqrt{3.69085}x50.2655} = 16.266217mm \tag{4.7}$$

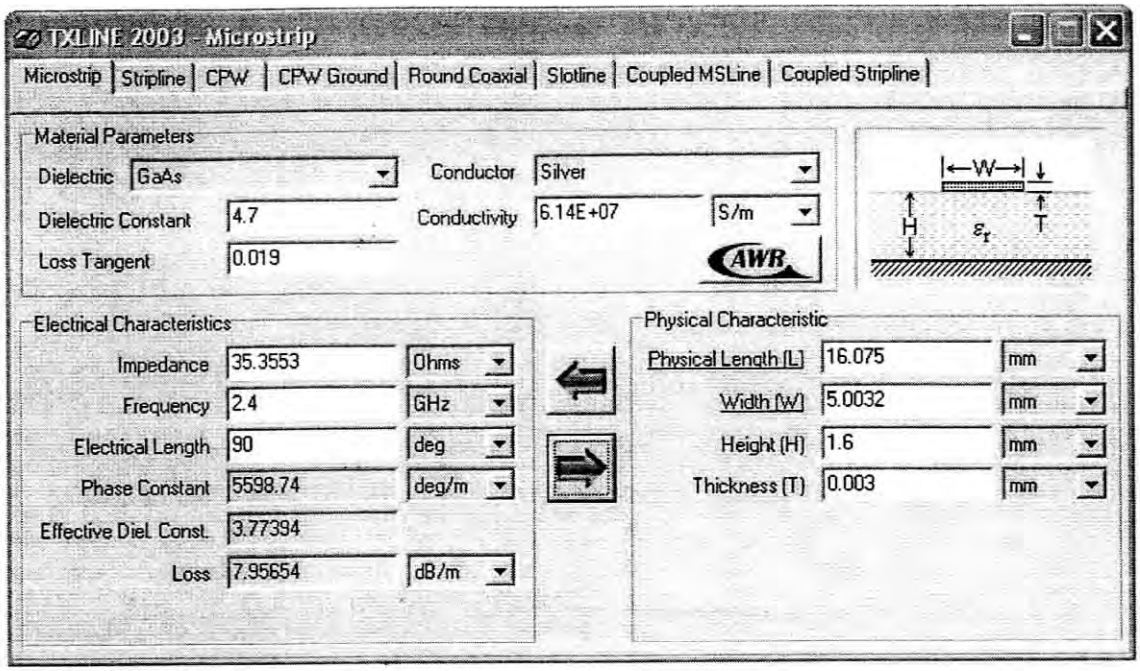

Figure A.2: Calculation Using TXLINE for $\frac{Z_o}{\sqrt{2}}$

Section B (For C and F)

$Z_o = 50\Omega$

$$B = \frac{377\pi}{2Z_o\sqrt{\varepsilon_r}} \tag{4.3}$$

$$= \frac{377\pi}{2x50\sqrt{4.7}} = 5.46631$$

$$\frac{W}{d} = \frac{2}{\pi}\left[B - 1 - \ln(2B-1) + \frac{\varepsilon_r - 1}{2\varepsilon_r}\left\{\ln(B-1) + 0.39 - \frac{0.61}{\varepsilon_r}\right\}\right] \tag{4.2}$$

$$= \frac{2}{\pi}\left[5.4631 - 1 - \ln(2x5.4631-1) + \frac{4.7-1}{2(4.7)}\left\{\ln(5.4631-1) + 0.39 - \frac{0.61}{4.7}\right\}\right]$$

$$= 1.8200086$$

$$W = 1.8200086x1.6mm \ = 2.912378mm$$

$$\varepsilon_{eff} = \frac{\varepsilon_r + 1}{2} + \frac{\varepsilon_r - 1}{4\sqrt{1 + \frac{12d}{w}}} \tag{4.1}$$

$$= \frac{4.7 + 1}{2} + \frac{4.7 - 1}{4\sqrt{1 + \frac{12(1.6mm)}{2.9121378mm}}} = 3.52137$$

$$k_o = \frac{2\pi f}{c} = \frac{2\pi(2.4GHz)}{3x10^8} = 50.2655m^{-1} \tag{4.6}$$

$$\ell = \frac{90°(\pi/180°)}{\sqrt{\varepsilon_{eff}}k_o} \tag{4.7}$$

$$= \frac{90°(\pi/180°)}{\sqrt{3.52137}x50.2655} = 16.65306mm$$

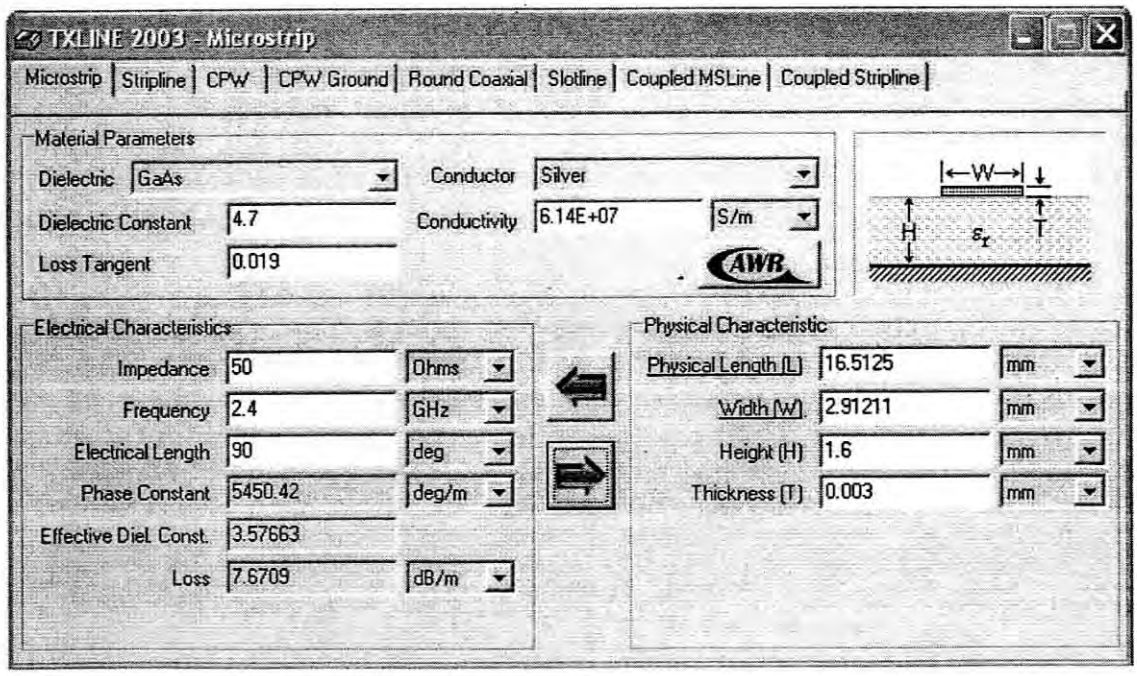

Figure A.3: Calculation Using TXLINE for $Z_o = 50\Omega$

APPENDIX B
CALCULATION AND SIMULATION OF CROSSOVER

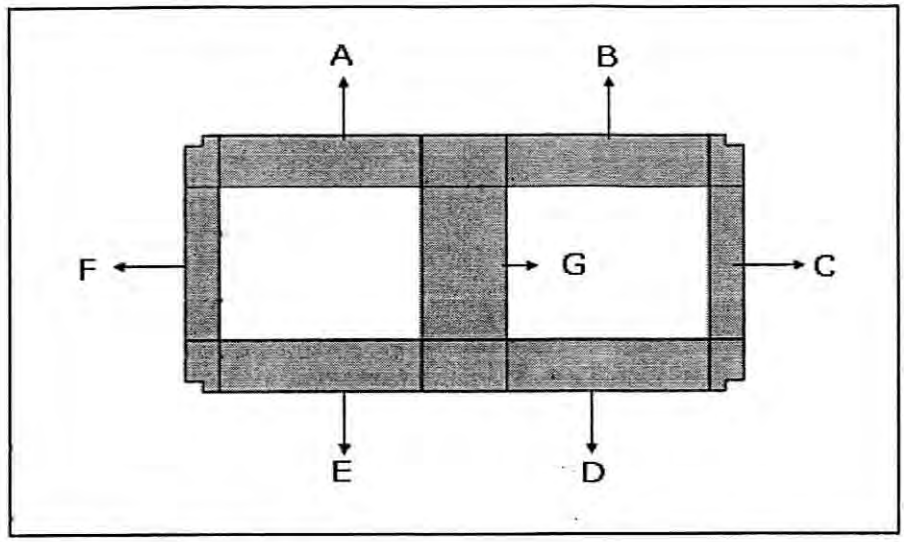

Figure B.1: General layout of the crossover

Frequency = 2.4GHz and Height (d) = 1.6mm

Section A (For A, B, D and E)

$$\frac{Z_o}{\sqrt{2}} = \frac{50}{\sqrt{2}} = 35.3553\Omega$$

$$B = \frac{377\pi}{2Z_o\sqrt{\varepsilon_r}} \qquad (4.3)$$

$$= \frac{377\pi}{2x35.3553\sqrt{4.7}} \quad = 7.72605$$

$$\frac{W}{d} = \frac{2}{\pi}\left[B - 1 - \ln(2B-1) + \frac{\varepsilon_r - 1}{2\varepsilon_r}\left\{\ln(B-1) + 0.39 - \frac{0.61}{\varepsilon_r}\right\}\right] \qquad (4.2)$$

$$= \frac{2}{\pi}\left[7.72605 - 1 - \ln(2x7.72605 - 1) + \frac{4.7-1}{2(4.7)}\left\{\ln(7.72605 - 1) + 0.39 - \frac{0.61}{4.7}\right\}\right]$$

$$= 3.124466mm$$

$$W = 3.124466x1.6mm \ = 4.99914mm$$

$$\varepsilon_{eff} = \frac{\varepsilon_r + 1}{2} + \frac{\varepsilon_r - 1}{4\sqrt{1 + \frac{12d}{w}}} \tag{4.1}$$

$$= \frac{4.7+1}{2} + \frac{4.7-1}{4\sqrt{1 + \frac{12(1.6mm)}{4.99914mm}}} = 3.69085$$

$$k_o = \frac{2\pi f}{c} = \frac{2\pi(2.4GHz)}{3x10^8} = 50.2655m^{-1} \tag{4.6}$$

$$\ell = \frac{90°(\pi/180°)}{\sqrt{\varepsilon_{eff}}k_o} \quad \frac{90°(\pi/180°)}{\sqrt{3.69085}x50.2655} = 16.266217mm \tag{4.7}$$

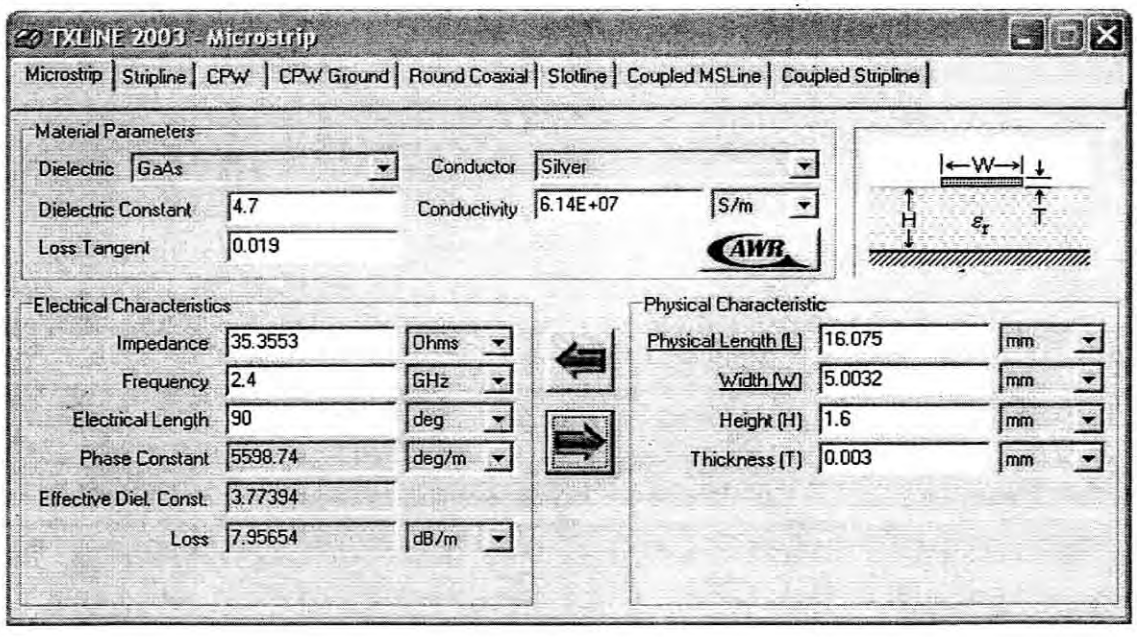

Figure B.2: Calculation Using TXLINE for $\frac{Z_o}{\sqrt{2}}$

Section B (For C and F)

$$Z_o = 50\Omega$$

$$B = \frac{377\pi}{2Z_o\sqrt{\varepsilon_r}} \tag{4.3}$$

$$= \frac{377\pi}{2x50\sqrt{4.7}} = 5.46631$$

$$\frac{W}{d} = \frac{2}{\pi}\left[B - 1 - \ln(2B-1) + \frac{\varepsilon_r - 1}{2\varepsilon_r}\left\{\ln(B-1) + 0.39 - \frac{0.61}{\varepsilon_r}\right\}\right] \tag{4.2}$$

$$= \frac{2}{\pi}\left[5.4631 - 1 - \ln(2x5.4631-1) + \frac{4.7-1}{2(4.7)}\left\{\ln(5.4631-1) + 0.39 - \frac{0.61}{4.7}\right\}\right]$$

$$= 1.8200086$$

$$W = 1.8200086x1.6mm = 2.912378mm$$

$$\varepsilon_{eff} = \frac{\varepsilon_r + 1}{2} + \frac{\varepsilon_r - 1}{4\sqrt{I + \frac{12d}{w}}} \tag{4.1}$$

$$= \frac{4.7+1}{2} + \frac{4.7-1}{4\sqrt{1 + \frac{12(1.6mm)}{2.9121378mm}}} = 3.52137$$

$$k_o = \frac{2\pi f}{c} = \frac{2\pi(2.4GHz)}{3x10^8} = 50.2655m^{-1} \tag{4.6}$$

$$\ell = \frac{90°(\pi/180°)}{\sqrt{\varepsilon_{eff}}k_o} \tag{4.7}$$

$$= \frac{90°(\pi/180°)}{\sqrt{3.52137}x50.2655} = 16.65306mm$$

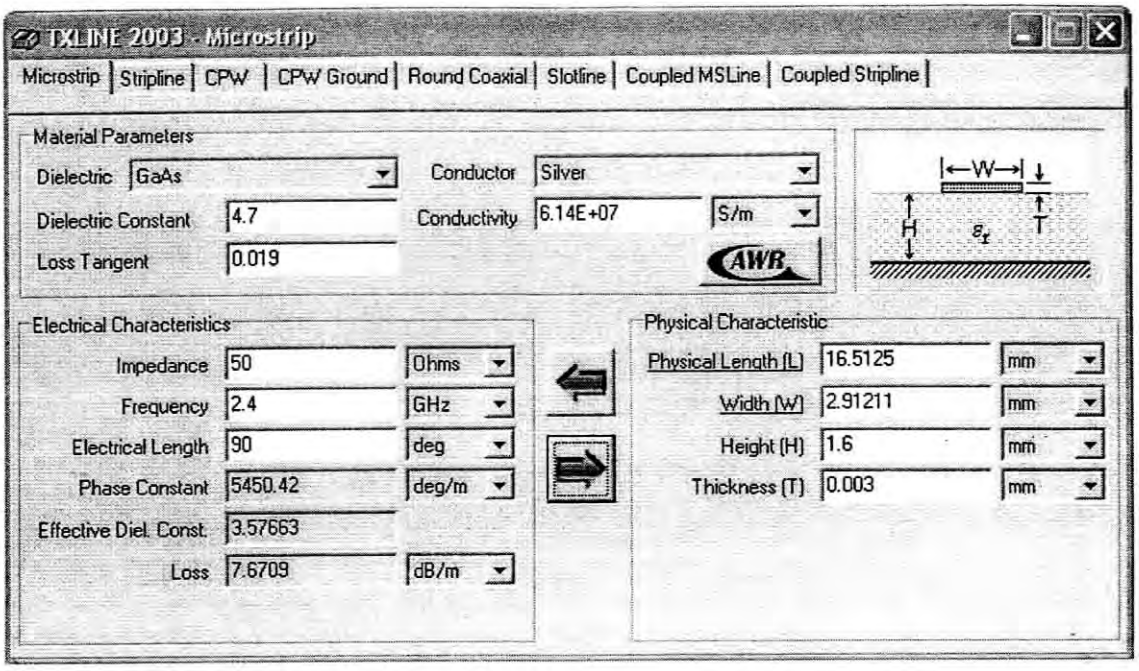

Figure B.3: Calculation Using TXLINE for $Z_o = 50\Omega$

Section B (For G)

$$\frac{Z_o}{2} = \frac{50}{2} = 25\Omega$$

$$B = \frac{377\pi}{2Z_o\sqrt{\varepsilon_r}} \tag{4.3}$$

$$= \frac{377\pi}{2x25\sqrt{4.7}} \quad = 10.9263$$

$$\frac{W}{d} = \frac{2}{\pi}\left[B - 1 - \ln(2B-1) + \frac{\varepsilon_r - 1}{2\varepsilon_r}\left\{\ln(B-1) + 0.39 - \frac{0.61}{\varepsilon_r}\right\}\right] \tag{4.2}$$

$$= \frac{2}{\pi}\left[10.9263 - 1 - \ln(2x10.9263 - 1) + \frac{4.7-1}{2(4.7)}\left\{\ln(10.9623 - 1) + 0.39 - \frac{0.61}{4.7}\right\}\right]$$

$$= 5.1242$$

$$W = 5..1242x1.6mm \quad = 8.19872mm$$

$$\varepsilon_{eff} = \frac{\varepsilon_r + 1}{2} + \frac{\varepsilon_r - 1}{4\sqrt{1 + \frac{12d}{w}}} \tag{4.1}$$

$$= \frac{4.7 + 1}{2} + \frac{4.7 - 1}{4\sqrt{1 + \frac{12(1.6mm)}{8.19872mm}}} = 3.45445$$

$$k_o = \frac{2\pi f}{c} = \frac{2\pi(2.4GHz)}{3x10^8} = 50.2655m^{-1} \tag{4.6}$$

$$\ell = \frac{90°(\pi/180°)}{\sqrt{\varepsilon_{eff}}k_o} \tag{4.7}$$

$$= \frac{90°(\pi/180°)}{\sqrt{3.45445}x50.2655} = 15.8621mm$$

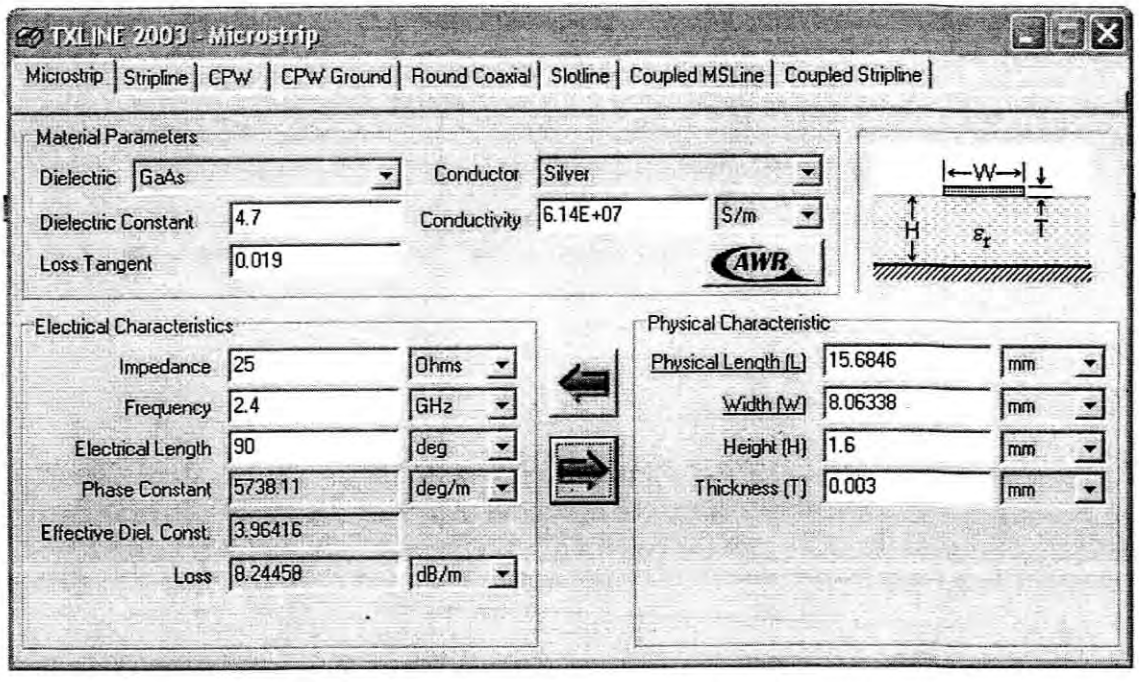

Figure B.4: Calculation Using TXLINE for $Z_0/2$